

Comprehensive determination of $^3J_{\text{HNH}\alpha}$ for unfolded proteins using $^{13}\text{C}'$ -resolved spin-echo difference spectroscopy

Renee Otten · Kathleen Wood · Frans A. A. Mulder

Received: 9 July 2009 / Accepted: 1 October 2009 / Published online: 7 November 2009
© The Author(s) 2009. This article is published with open access at Springerlink.com

Abstract An experiment is presented to determine $^3J_{\text{HNH}\alpha}$ coupling constants, with significant advantages for applications to unfolded proteins. The determination of coupling constants for the peptide chain using 1D ^1H , or 2D and 3D ^1H - ^{15}N correlation spectroscopy is often hampered by extensive resonance overlap when dealing with flexible, disordered proteins. In the experiment detailed here, the overlap problem is largely circumvented by recording ^1H - $^{13}\text{C}'$ correlation spectra, which demonstrate superior resolution for unfolded proteins. J-coupling constants are extracted from the peak intensities in a pair of 2D spin-echo difference experiments, affording rapid acquisition of the coupling data. In an application to the cytoplasmic domain of human neuroligin-3 (hNlg3 $_{\text{cyt}}$) data were obtained for 78 residues, compared to 54 coupling constants obtained from a 3D HNHA experiment. The coupling constants suggest that hNlg3 $_{\text{cyt}}$ is intrinsically disordered, with little propensity for structure.

Keywords J-coupling · Conformation · IDP · IUP · HNHA

Disordered proteins attract increasing attention, due in part to the fact that intrinsic disorder is prevalent in the proteomes of higher order organisms (Ward et al. 2004). In addition, it has been established that the disordered states

of proteins are not mere featureless ‘random coils’, but are characterized by secondary structure propensities of the polypeptide backbone, sometimes augmented with specific local interactions between side chains (Dill and Shortle 1991; Mittag and Forman-Kay 2007; Shortle 1996; Wirmer et al. 2005). High-resolution determination of residual structure in these inherently flexible molecules is therefore necessary (Bartlett and Radford 2009). NMR spectroscopy is undoubtedly the most appropriate technique to offer detailed insight into disordered states, being sensitive to the length and time scales characterizing the atomic structure (Bartlett and Radford 2009; Eliezer 2009; Mulder et al. 2009; Wirmer et al. 2005). In our analyses of intrinsically disordered proteins (IDPs) we have been interested in the measurement of scalar coupling constants to probe the local polypeptide backbone structure. To this end we have employed experiments that have been very successfully applied to folded proteins, and for which careful parameterization of three-bond coupling constants as a function of the backbone angle ϕ are available (Billeter et al. 1992; Case et al. 2000; Vuister and Bax 1993). For example, the most effectual and widely used coupling constants to define the backbone geometry, $^3J_{\text{HNH}\alpha}$, can be determined efficiently from a pair of 2D spin-echo difference measurements, obtained as HMQC (Ponstingl and Otting 1998) or HSQC (Petit et al. 2002) variants, recorded on ^{15}N -labeled proteins. 2D ^1H - ^{15}N correlation spectra of unfolded proteins are, however, severely compromised by resonance overlap, thereby limiting the number of probes available for conformational analysis. Since 3D experiments (Kuboniwa et al. 1994; Vuister and Bax 1993) to measure $^3J_{\text{HNH}\alpha}$ include the 2D ^1H - ^{15}N correlations as ‘diagonal peaks’, overlap in the 2D spectrum comparatively reduces the utility of 3D spectroscopy for the measurement of $^3J_{\text{HNH}\alpha}$ in unfolded proteins. In an elegant approach, Lendel

Renee Otten and Kathleen Wood contributed equally to this work.

R. Otten · K. Wood · F. A. A. Mulder (✉)
Department of Biophysical Chemistry, Groningen Biomolecular Sciences and Biotechnology Institute, University of Groningen, Nijenborgh 4, 9747 AG Groningen, The Netherlands
e-mail: f.a.a.mulder@rug.nl
URL: Homepage: www.rug.nl/gbb/nmr

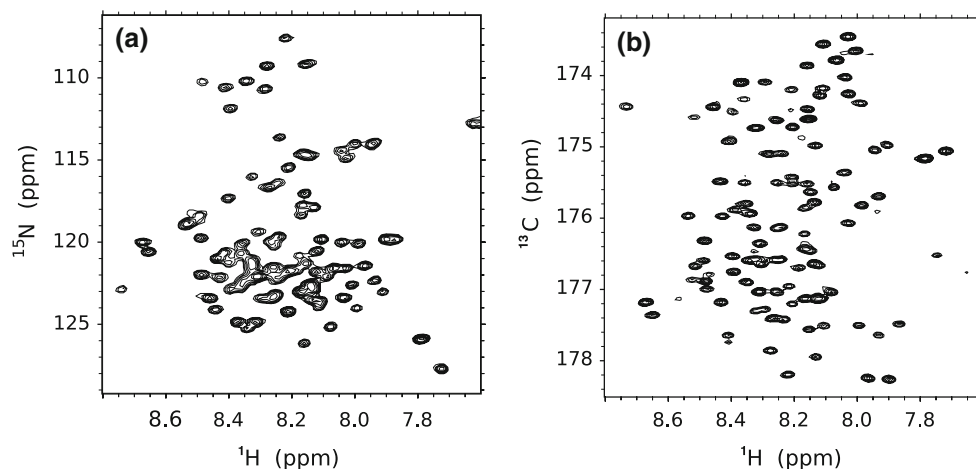
and Damberg (2009) very recently showed that improved resolution can be obtained by effectively removing the homonuclear coupling from the proton linewidth in a 3D J-resolved ^1H - ^{15}N correlation spectrum, and were thereby able to achieve a near-complete analysis of the coupling constants for the natively disordered protein alpha-synuclein. In this paper we present an alternative approach to achieve excellent spectral resolution, which is based on 2D spectroscopy.

We show here that a much more complete set of $^3J_{\text{HNH}\alpha}$ coupling constants can be obtained for uniformly (^{15}N , ^{13}C)-labeled proteins by recording $^{13}\text{C}'$, rather than ^{15}N , chemical shift modulation in the indirectly detected domain. The rationale for this strategy was derived from a comparison of 2D ^1H - ^{15}N and ^1H - $^{13}\text{C}'$ correlation spectra (*viz.* Fig. 1) for the cytoplasmic domain of human neuroigin-3 (hNlg3cyt), obtained with gradient-sensitivity enhanced HSQC (Kay et al. 1992) and HNC0 (Yang and Kay 1999) experiments, respectively. Both experiments were recorded with 100 complex time points in the indirect dimension, and processed identically. Figure 1 clearly demonstrates the improvement in resolution that is obtained in the ^1H - $^{13}\text{C}'$ spectrum of the unfolded protein, compared to ^1H - ^{15}N correlation spectroscopy. In addition to the higher apparent spread of the signals in the ^1H - $^{13}\text{C}'$ spectrum, the $^{13}\text{C}'$ line widths (measured at 14.1 T) are also significantly smaller. For example, in the case of hNlg3cyt, the natural line widths measured in ^1H - $^{13}\text{C}'$ and ^1H - ^{15}N spectra were 5.6 and 16.2 Hz, respectively.

With the high resolution of ^1H - $^{13}\text{C}'$ correlation spectroscopy in mind we developed a novel pulse sequence to measure $^3J_{\text{HNH}\alpha}$ for uniformly ^{15}N , ^{13}C -enriched proteins, which is shown in Fig. 2. The scheme is a combination of HNC0 triple resonance spectroscopy (Yang and Kay 1999) and HMQC-based spin-echo difference $^3J_{\text{HNH}\alpha}$ experiments (Ponstingl and Otting 1998): through successive INEPT transfer steps the starting amide polarization is transferred

to $^{13}\text{C}'$ for chemical shift encoding. The sequence of events up to point *a* can be described as $\text{H}_Z \rightarrow 2\text{N}_Z\text{C}'_Z$, and, after a 90° $^{13}\text{C}'$ pulse is followed by carbonyl carbon chemical shift encoding. Subsequently, at point *b* in the sequence, evolution of the anti-phase term $-2\text{N}_Y\text{C}'_Z$ takes place under the one-bond ^{15}N - $^{13}\text{C}'$ and ^{15}N - ^1H coupling Hamiltonians simultaneously. After a delay $\kappa = 1/(2J_{\text{NC}'\kappa})$ the density operator is proportional to $4\text{H}_Z\text{N}_X\text{C}'_Z \cdot \cos(\pi J_{\text{NC}'\kappa}) + 2\text{H}_Z\text{N}_Y \cdot \sin(\pi J_{\text{NC}'\kappa})$. A 90° ^1H pulse transforms this into $-4\text{H}_Y\text{N}_X\text{C}'_Z \cdot \cos(\pi J_{\text{NC}'\kappa}) - 2\text{H}_Y\text{N}_Y \cdot \sin(\pi J_{\text{NC}'\kappa})$, which interrupts any further evolution under the proton-nitrogen coupling, while allowing now for the simultaneous evolution under the one-bond $^{13}\text{C}'$ - ^{15}N and three-bond $^1\text{H}^{\text{N}}$ - $^1\text{H}^{\alpha}$ coupling Hamiltonians. At point *c* in the sequence the refocusing due to $J_{\text{NC}'}$ is complete. Subsequently, after the final 90° ^{15}N pulse, evolution under the mutual scalar coupling for a period κ also completely refocuses the nitrogen-proton anti-phase terms. A non-selective 180° proton pulse in the middle of the multiple quantum (MQ) evolution period ensures that ^1H chemical shift evolution is fully refocused. In total, evolution due to the $^3J_{\text{HNH}\alpha}$ coupling equals $2T$ at that point. After the last 90° ^1H pulse the only terms present are now $\text{H}_X \cdot \cos(\pi J_{\text{HNH}\alpha} 2T) - 2\text{H}_Z\text{H}_Y \cdot \sin(\pi J_{\text{HNH}\alpha} 2T)$. Only the in-phase term survives the subsequent echo period, which is comprised of an amide proton-selective REBURP refocusing pulse (Geen and Freeman 1991), combined with a gradient echo. This short additional element is also necessary to suppress any small amount of water magnetization that is not returned to the $+Z$ axis by the last 90° ^1H pulse in the sequence. Fourier transformation leads to an absorptive signal at the amide proton chemical shift, with its intensity encoding the three-bond $^1\text{H}^{\text{N}}$ - $^1\text{H}^{\alpha}$ coupling constant. In order to quantify the $^3J_{\text{HNH}\alpha}$ coupling constants a reference measurement is performed, during which selective inversion of $^1\text{H}^{\alpha}$ is achieved at time points $T/2 (= 1/(4 \times J_{\text{NC}'})$) and $3T/2 (= 3/(4 \times J_{\text{NC}'})$), thereby effectively refocusing the coupling (these pulses are shown as boxed filled domes in Fig. 2). For

Fig. 1 2D ^1H - ^{15}N HSQC (a) and ^1H - $^{13}\text{C}'$ H(N)CO (b) correlation spectra for the 139 amino acid construct of the intrinsically disordered protein domain hNlg3cyt



this purpose, IBURP-2 pulses (Geen and Freeman 1991) were employed, which effect a rapid inversion during the central segment of the pulse. Practically, two experiments are recorded: one with the selective $^1\text{H}^z$ pulses (I_A) and one without (I_B). Residue-specific values for the three-bond coupling constants are calculated from the intensity ratios of the resulting spectral signals as $^3J_{\text{HNH}^z} = (2\pi T)^{-1} \text{acos}(I_B/I_A)$.

A few further aspects of the experiment are worth mentioning at this point. First, during the final part of the pulse sequence, no sensitivity losses incur from the refocusing of $-2N_Y C'_Z$ during the 2T period of 33 ms. The MQ evolution period nicely combines the refocusing period with the period that is required for the three-bond proton-proton coupling evolution, since these two processes require approximately the same amount of time.

Second, ^1H composite pulse decoupling is applied during $^{13}\text{C}'$ evolution, since three-bond couplings to β -protons (2–6 Hz) would otherwise contribute to unresolved line-broadening. Under these conditions narrow lines are observed for $^{13}\text{C}'$, due to the absence of strong relaxation mechanisms: the dominant source of relaxation, even at moderate static magnetic field strength, is the chemical shift anisotropy (CSA), which is modest at 14.1 T. Since protons are far removed from the carbonyl carbon atom, dipolar relaxation contributions are small. For unfolded proteins a three-fold reduction in the line widths was

observed by recording $^{13}\text{C}'$ rather than ^{15}N -resolved spectra (see above), and this advantage also extends to folded proteins: for calbindin D_{9k} the average carbonyl line width is 6.4 Hz, compared with 20.0 Hz for nitrogen. In addition, the high spectral dispersion displayed by $^{13}\text{C}'$ arises from the fact that the carbonyl chemical shift is influenced by the neighboring residue types to both sides (Wang and Jardetzky 2002; Wishart et al. 1995; Yao et al. 1997). The favorable relaxation properties and sequence-specific shielding contributions together ensure the high inherent resolution for ^1H - $^{13}\text{C}'$ correlation spectroscopy displayed by disordered proteins.

Third, a water flip-back strategy is used to avoid the transfer of water saturation to the solvent-exposed, exchangeable amide protons. Since all amides in the unfolded state are solvent-exposed, care has to be taken to control the state of water throughout the pulse sequence. Failure to establish that the water polarization is very similar in each of the two spin-echo difference experiments could lead to significant systematic errors. A three-pronged approach was taken here: (1) Since radiation damping can rapidly cause the large out-of-equilibrium water polarization to align with the external magnetic field we have limited the time during which it is not aligned along the +Z axis; (2) During the chemical shift evolution period where the water polarization is along -Z, weak gradients are employed to rapidly dephase any magnetization that rotates away from the -Z axis; (3) When the magnetization is in

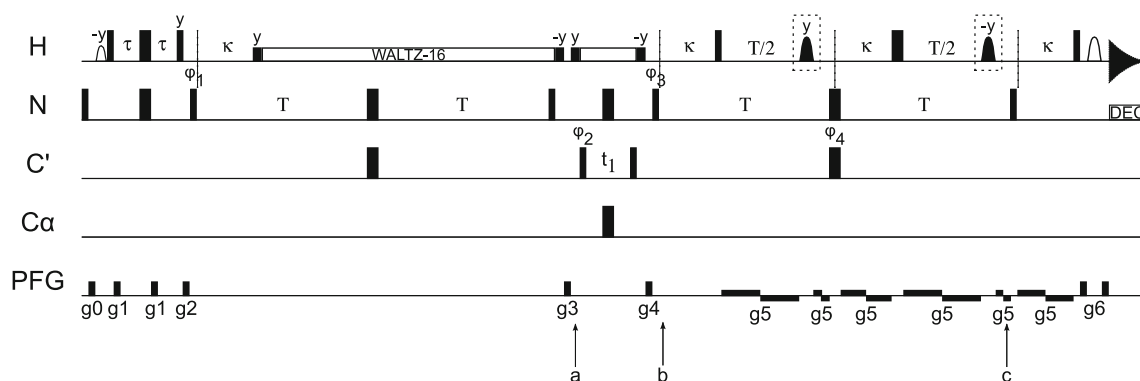


Fig. 2 Pulse sequence of the $^{13}\text{C}'$ -resolved spin-echo difference experiment to measure $^3J_{\text{HNH}^z}$. Two versions of the experiment are executed, one with the boxed inversion pulses present (A) and one without (B). Narrow (wide) filled bars indicate 90° (180°) RF pulses applied along the x-axis, unless otherwise indicated. The ^1H carrier is centered at the water resonance (4.76 ppm) and proton pulses are applied with a field strength of $\omega_1/2\pi = 37.3$ kHz. Proton decoupling is achieved using a WALTZ-16 decoupling scheme with $\omega_1/2\pi = 5.0$ kHz. The water flip-back pulse at the beginning of the sequence has an EBURP-1 profile (Geen and Freeman 1991) ($\omega_1/2\pi = 715$ Hz, 5.12 ms duration). The filled dome shaped proton pulses are used for the selective inversion of the $^1\text{H}^z$ region and have an IBURP-2 profile ($\omega_1/2\pi = 1.75$ kHz, 2.9 ms duration). The open dome shaped proton pulse has a REBURP profile and inverts only the amide

region ($\omega_1/2\pi = 1.55$ kHz, 4.01 ms duration) through phase-modulation. The ^{15}N carrier is centered at 117 ppm and nitrogen pulses are applied with a field strength of $\omega_1/2\pi = 6.0$ kHz. Rectangular 90° (180°) ^{13}C pulses are applied with a field of $\omega_1/2\pi = \Delta/\sqrt{15}$ ($\Delta/\sqrt{3}$), where Δ is the difference (in Hz) between $^{13}\text{C}^\alpha$ (57 ppm) and $^{13}\text{C}'$ (176 ppm). Decoupling during acquisition is done using GARP-1, with $\omega_1/2\pi = 1.25$ kHz. Values of the delays are: $\tau = 2.3$ ms, $\kappa = 5.4$ ms, $T = 16.67$ ms. Gradient strengths in G/cm (length in ms): $g_0 = 8.0$ (0.5), $g_1 = 5.0$ (0.5), $g_2 = 15.0$ (2.0), $g_3 = 20.0$ (0.75), $g_4 = 15.0$ (2.0), $g_5 = 1.0$ (variable), $g_6 = 21.0$ (0.1). Phase cycling: $\phi_1 = x$; $\phi_2 = [x, -x]$; $\phi_3 = [x, x, -x, -x]$; $\phi_4 = [x, -x]$; $\phi_{\text{receiver}} = [x, -x, -x, x]$. Quadrature detection in F_1 is obtained by incrementing ϕ_2 , according to the States-TPPI protocol

the transverse plane it is kept locked by a strong ($\omega_1/2\pi \sim 5$ kHz) rotating transverse field, which is simultaneously used for composite pulse ^1H decoupling. Residual water suppression after the final 90° ^1H pulse is achieved by a selective $^1\text{H}^{\text{N}}$ REBURP refocusing pulse (Geen and Freeman 1991), bracketed by gradients, akin to the WATERGATE procedure (Piotto et al. 1992). Rather than judging the effectiveness of the water flip-back procedure from the degree of water suppression, an optional 90° ^1H pulse was included at the end of the pulse sequence to query the longitudinal water polarization prior to acquisition. This was done, by comparing the signal intensity with that obtained after a single 90° ^1H pulse. To avoid receiver overflow, the signal was moderated, by placing a 6 dB attenuator between the preamplifier and the observation receiver (i.e. prior to signal digitization). In this way it was established that the flip-back strategy was effective to 95% or better. More importantly, the water state was no different in the experiments that do or do not contain selective $^1\text{H}^{\text{z}}$ decoupling pulses. We found that this procedure yielded more reliable estimates of the water signal magnitude, than using a short tapping pulse.

To benchmark the experimental procedure, the new pulse sequence was first applied to the small folded protein calbindin $\text{D}_{9\text{k}}$, and measured $^3J_{\text{HNH}^{\text{z}}}$ values were compared with coupling constants derived from a 3D HNHA experiment (Vuister and Bax 1993). The 3D data set was recorded using 47×62 complex data points for the proton and nitrogen domain, corresponding to maximum evolution times of 5.9 and 31.9 ms, respectively. Linear prediction was used in both indirect domains, followed by strongly apodizing window functions. The coupling constants extracted using this procedure were the same as those obtained without linear prediction. The total acquisition time was 30 h. For the 2D measurement 256 complex points were acquired in the $^{13}\text{C}'$ domain, using a maximum evolution time of 170.7 ms. A pair of experiments (once with and once without modulation due to the three-bond coupling) was recorded in 6 h, and this procedure was repeated four times, in an interleaved fashion, to ensure that any changes would affect both experiments equally, and the data subsequently added together.

As Fig. 3a shows, there is excellent agreement between the coupling constants for this protein, derived from 2D and 3D measurements, except for the presence of a systematic difference between the two datasets. Coupling constants obtained for ten residues for which the selective pulses do not perfectly effect the desired inversion of $^1\text{H}^{\text{z}}$ magnetization, or completely refocus the $^1\text{H}^{\text{N}}$ region were excluded from the analysis, and Fig. 3a. For example, $^3J_{\text{HNH}^{\text{z}}}$ values for Leu31 and Phe63 appeared seriously underestimated in the 2D measurement. This outcome was anticipated, as the $^1\text{H}^{\text{z}}$ chemical shifts for Leu31 and Phe63

are 2.37 and 3.32 ppm, respectively, and fall outside the region for proper inversion.

Although differential relaxation of the in-phase and anti-phase terms in the 3D HNHA scalar coupling measurement may lead to the systematic underestimation of the true J values for larger proteins (Harbison 1993; Kuboniwa et al. 1994; Vogeli et al. 2007), the short rotational correlation time for calbindin $\text{D}_{9\text{k}}$ ($\tau_{\text{C}} = 4.2$ ns) suggests that a correction for differential relaxation would amount to underestimations of the true J couplings by approximately 5% (Kuboniwa et al. 1994). Even after making this correction it appears that the values from the 3D HNHA experiment underestimate the scalar coupling values by about 0.5 Hz. Interestingly, Wang and Bax (Wang and Bax 1996) required a similar systematic increase of 3D HNHA-derived relaxation-corrected $^3J_{\text{HNH}^{\text{z}}}$ values for human ubiquitin (0.4 Hz) to obtain satisfactory agreement with values obtained using 2D J-modulated CT-HMQC spectra and HNCA[HA]-E.COSY experiments. It therefore appears that the J couplings measured with the proposed 2D spin-echo difference scheme are robust, even for small folded proteins.

The experimental coupling constants were compared with those calculated from a 1.6 Å X-ray crystal structure 4ICB (Svensson et al. 1992), using the Karplus parametrization by Vuister and Bax (Vuister and Bax 1993). The agreement with the 2D spin-echo difference derived coupling constants is very good, although there are a number of residues for which the coupling constants are further removed from the calculated curve than would be expected from the quality of the data. There exist two explanations for these differences. The first reason is that values for $^3J_{\text{HNH}^{\text{z}}}$ calculated from a single static structure cannot be expected to faithfully represent experimental data in the case of dynamics. Residues that are known to be flexible from NMR relaxation studies (Kördel et al. 1992) indeed show poor agreement. For example, residues belonging to the termini (Glu4, Lys72-Ser74) and the linker region (Lys41) yield values between 6 and 8 Hz, indicative of averaging, and are more than 1 Hz removed from the values calculated from a static structure. Second, a number of further deviations appear to be the result of true differences between the structures in the crystal lattice and in solution. Calbindin $\text{D}_{9\text{k}}$ contains two loops, which coordinate a calcium ion each, providing backbone as well as side chain oxygen ligands. The first loop comprises Ala14-Glu27, and the second extends from Asp54 to Glu65. It is observed that data for residues of the four helices nicely fit to the Karplus relation, whereas the experimentally determined J couplings for all other residues that deviate by more than 1 Hz from calculation map to the two calcium binding loops. These are indicated in Fig. 3b. It appears that backbone angles in the loop regions

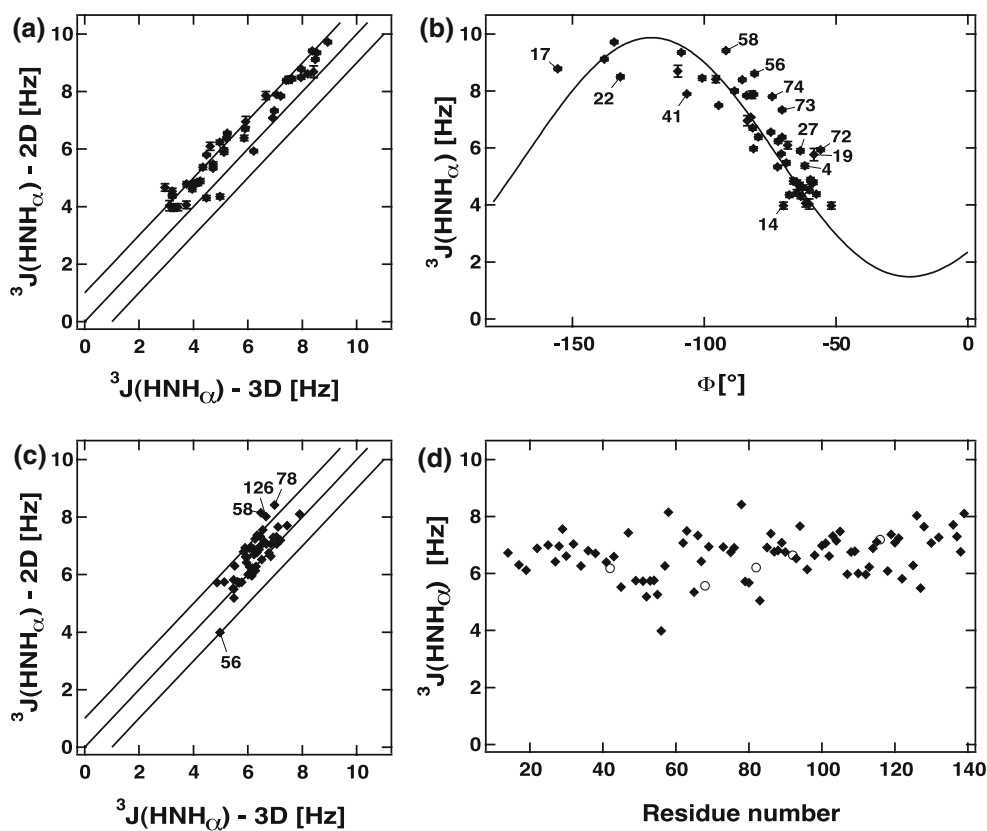


Fig. 3 **a** Comparison of experimental ${}^3J_{\text{HNH}\alpha}$ coupling constants for the small folded protein calbindin D_{9k}, obtained using 2D ${}^1\text{H}$ - ${}^{13}\text{C}'$ spin-echo difference and 3D HNHA experiments. *Error bars* on the 3D data set are similar to the size of the symbols, and are not shown for clarity. **b** Comparison of the experimental 2D ${}^1\text{H}$ - ${}^{13}\text{C}'$ spin-echo difference derived ${}^3J_{\text{HNH}\alpha}$ coupling constants for calbindin D_{9k} with those calculated from the 1.6 Å X-ray crystal structure (Svensson et al. 1992) 4ICB, using the Karplus parametrization by Vuister and Bax (Vuister and Bax 1993). **c** Comparison of experimental ${}^3J_{\text{HNH}\alpha}$

coupling constants for the intrinsically disordered protein domain hNlg3cyt, obtained using 2D ${}^1\text{H}$ - ${}^{13}\text{C}'$ spin-echo difference and 3D HNHA experiments. *Error bars* are of similar size as the sample points. **d** ${}^3J_{\text{HNH}\alpha}$ coupling constants for the intrinsically disordered protein domain hNlg3cyt, obtained with the new pulse sequence. *Error bars* are smaller than the size of the symbol for most data points. *Empty circles* show 3D HNHA-derived coupling constants for five additional residues, which give rise to overlapped cross peaks in the 2D ${}^1\text{H}$ - ${}^{13}\text{C}'$, but not in the 2D ${}^1\text{H}$ - ${}^{15}\text{N}$ spectrum

differ by up to 10° between the crystalline and solution states. This assertion is confirmed by ${}^3J_{\text{C}'\text{C}'}$ couplings, which report on the same dihedral angle (data not shown).

Once the methodology was validated, we applied the experiment to the disordered protein domain hNlg3cyt. In a previous study the structural nature of this domain was studied by a host of biophysical methods, including small-angle X-ray scattering, CD spectroscopy and NMR spectroscopy (Paz et al. 2008). The main conclusion of that work was that hNlg3cyt belongs to the family of intrinsically disordered proteins (IDPs), also referred to as natively unfolded proteins. Since no NMR assignments were available at the time of that study, the experimental data were used to derive an overall picture of the protein's physical state. Meanwhile we have obtained near-complete backbone resonance assignments of the protein, such that a site-specific analysis of order and disorder in the sequence can be undertaken. Because scalar coupling constants are very sensitive to the local order of the peptide bond, they

would serve as excellent probes to detect any residual structural propensity along the polypeptide chain.

Using the 3D HNHA experiment, a dataset of 46×62 complex data points was collected for the proton and nitrogen domain, corresponding to maximum evolution times of 5.7 and 31.9 ms, respectively. The total measuring time was 30 h. Due to extensive overlap we were only able to obtain 54 ${}^3J_{\text{HNH}\alpha}$ values for hNlg3cyt from this dataset. Therefore the pulse sequence of Fig. 2 was employed, using 128 complex data points for the ${}^{13}\text{C}'$ dimension, with a maximum evolution time of 160.0 ms. The experiments with and without ${}^1\text{H}^\alpha$ decoupling were repeated four times. The total measuring time was 30 h. Making use of the 2D ${}^1\text{H}$ - ${}^{13}\text{C}'$ correlation spectra, the number of probes amenable to analysis increased to 78, out of 105 possible (139-residue long sequence, with 10 amino acids in the poly-histidine tag, 16 proline and 8 glycine residues). Of note, for unfolded proteins the clear separation of the narrow ${}^1\text{H}^\alpha$ (4.0–4.8 ppm) and ${}^1\text{H}^{\text{N}}$ (7.9–8.7 ppm) chemical shift

ranges does not hinder the coupling measurement as it does for folded proteins (see above), and no data needed to be excluded from further analysis. A single outlier was obtained (residue 56), but the reason for this discrepancy is currently unknown.

The ${}^3J_{\text{HNH}\alpha}$ values measured for hNlg3cyt by 3D HNHA and 2D spin-echo difference spectroscopy are compared in Fig. 3c. Since the inter-proton dipolar correlation times in unfolded proteins are much smaller than those of folded proteins, it is unlikely that the effects due to differential relaxation need to be taken into account (Harbison 1993; Kuboniwa et al. 1994; Rexroth et al. 1995). However, a small systematic difference of about 0.4 Hz is still observed, as was the case for calbindin D_{9k}. Such a systematic difference has previously been attributed to an underestimation of the coupling constants using the 3D HNHA experiment, suggesting that the values derived with the new experiment are reliable. In addition, since the 2D spin-echo difference-derived coupling constants agree well with the three-dimensional molecular structure for calbindin D_{9k}, ${}^3J_{\text{HNH}\alpha}$ values for unfolded proteins can be used as reliable probes of polypeptide conformation.

A plot of the measured ${}^3J_{\text{HNH}\alpha}$ for hNlg3cyt as a function of residue number is shown in Fig. 3d. The average value of ca. 7 Hz is similar to values obtained for flexible peptides and other disordered peptides, corroborating earlier results (Paz et al. 2008). However, a few regions deviate from this trend, showing significantly lower values. The interpretation of this result is that conformations with values for the angle ϕ towards -60° are increasingly being populated. Importantly, from ${}^3J_{\text{HNH}\alpha}$ values alone it is not possible to say whether these include canonical α -helical or polyproline type II (PPII) structures. This will await further investigation, and an analysis of additional experimental data is beyond the scope of this Communication, and will be presented elsewhere.

In summary, an experiment is presented to measure ${}^3J_{\text{HNH}\alpha}$, employing ${}^{13}\text{C}'$ - instead of ${}^{15}\text{N}$ -resolved experiments. The sizeable gain in the number of probes that become available for unfolded proteins suggests that the proposed experiment serves as an important complement to characterize the structure and dynamics of disordered states of proteins.

Acknowledgments We thank Dr. Aviv Paz and Prof. Joel Sussman (Weizmann Institute, Rehovot, Israel) for the sample used in this study. K. W. acknowledges a post-doctoral fellowship from the European Molecular Biology Organization (EMBO). This work was supported by a VIDI grant to F.A.A.M. from the Netherlands Organization for Scientific Research (NWO).

Open Access This article is distributed under the terms of the Creative Commons Attribution Noncommercial License which permits any noncommercial use, distribution, and reproduction in any medium, provided the original author(s) and source are credited.

References

- Bartlett AI, Radford SE (2009) An expanding arsenal of experimental methods yields an explosion of insights into protein folding mechanisms. *Nature Struct Mol Biol* 16(6):582–588
- Billeter M, Neri D, Otting G, Qian YQ, Wuthrich K (1992) Precise vicinal coupling constants ${}^3J_{\text{HNH}\alpha}$ in proteins from nonlinear fits of J-modulated [N-15, H-1]-COSY experiments. *J Biomol NMR* 2(3):257–274
- Case DA, Scheurer C, Bruschweiler R (2000) Static and dynamic effects on vicinal scalar J couplings in proteins and peptides: a MD/DFT analysis. *J Am Chem Soc* 122(42):10390–10397
- Dill KA, Shortle D (1991) Denatures states of proteins. *Ann Rev Biochem* 60:795–825
- Eliezer D (2009) Biophysical characterization of intrinsically disordered proteins. *Curr Opin Struct Biol* 19(1):23–30
- Geen H, Freeman R (1991) Band-selective radiofrequency pulses. *J Magn Reson* 93(1):93–141
- Harbison GS (1993) Interference between J-couplings and cross-relaxation in solution NMR spectroscopy: consequences for macromolecular structure determination. *J Am Chem Soc* 115(7):3026–3027
- Kay LE, Keifer P, Saarinen T (1992) Pure absorption gradient enhanced heteronuclear single quantum correlation spectroscopy with improved sensitivity. *J Am Chem Soc* 114(26):10663–10665
- Kördel J, Skelton NJ, Akke M, Palmer AG, Chazin WJ (1992) Backbone dynamics of calcium-loaded calbindin D9k studied by 2-dimensional proton-detected N-15 NMR-spectroscopy. *Biochemistry* 31(20):4856–4866
- Kuboniwa H, Grzesiek S, Delaglio F, Bax A (1994) Measurement of HN-Halpa J-couplings in calcium-free calmodulin using new 2D and 3D water flip-back methods. *J Biomol NMR* 4(6):871–878
- Lendel C, Damberg P (2009) 3D J-resolved NMR spectroscopy for unstructured polypeptides: fast measurement of $({}^3J_{\text{HNH}\alpha})$ coupling constants with outstanding spectral resolution. *J Biomol NMR* 44(1):35–42
- Mittag T, Forman-Kay JD (2007) Atomic-level characterization of disordered protein ensembles. *Curr Opin Struct Biol* 17(1):3–14
- Mulder FAA, Lundqvist M, Scheek RM (2009) Nuclear magnetic resonance spectroscopy applied to (intrinsically) disordered proteins. In: Uversky V, Longhi S (eds) *Assessing structures and conformations of intrinsically disordered proteins*. John Wiley and Sons, New Jersey
- Paz A, Zeev-Ben-Mordehai T, Sherman E et al (2008) Biophysical characterization of the unstructured cytoplasmic domain of the human neuronal adhesion protein neuroligin 3. *Biophys J* 95(4):1928–1944
- Petit A, Vincent SJF, Zwahlen C (2002) Cosine modulated HSQC: a rapid determination of $({}^3J_{\text{HNH}\alpha})$ scalar couplings in N-15-labeled proteins. *J Magn Reson* 156(2):313–317
- Piotto M, Saudek V, Sklenar V (1992) Gradient-tailored excitation for single-quantum NMR-spectroscopy of aqueous solutions. *J Biomol NMR* 2(6):661–665
- Ponstingl H, Otting G (1998) Rapid measurement of scalar three-bond H-1(N)-H-1(alpha) spin coupling constants in N-15-labelled proteins. *J Biomol NMR* 12(2):319–324
- Rexroth A, Schmidt P, Szalma S, Geppert T, Schwalbe H, Griesinger C (1995) New principles for the determination of coupling constants that largely suppresses differential relaxation effects. *J Am Chem Soc* 117(41):10389–10390
- Shortle DR (1996) Structural analysis of non-native states of proteins by NMR methods. *Curr Opin Struct Biol* 6(1):24–30
- Svensson LA, Thulin E, Forsén S (1992) Proline cis-trans isomers in calbindin D9k observed by X-ray crystallography. *J Mol Biol* 223(3):601–606

- Vogeli B, Ying JF, Grishaev A, Bax A (2007) Limits on variations in protein backbone dynamics from precise measurements of scalar couplings. *J Am Chem Soc* 129(30):9377–9385
- Vuister GW, Bax A (1993) Quantitative J correlation—a new approach for measuring homonuclear 3-bond J(HNH α) couplings—constants in N-15 enriched proteins. *J Am Chem Soc* 115(17):7772–7777
- Wang AC, Bax A (1996) Determination of the backbone dihedral angles phi in human ubiquitin from reparametrized empirical Karplus equations. *J Am Chem Soc* 118(10):2483–2494
- Wang YJ, Jardetzky O (2002) Investigation of the neighboring residue effects on protein chemical shifts. *J Am Chem Soc* 124(47):14075–14084
- Ward JJ, Sodhi JS, McGuffin LJ, Buxton BF, Jones DT (2004) Prediction and functional analysis of native disorder in proteins from the three kingdoms of life. *J Mol Biol* 337(3):635–645
- Wirmer J, Schlörb C, Schwalbe H (2005) Conformation and dynamics of nonnative states of proteins studied by NMR spectroscopy. In: Buchner J, Kiefhaber T (eds) *Protein folding handbook part I*. Wiley-VCH, Weinheim, pp 737–808
- Wishart DS, Bigam CG, Holm A, Hodges RS, Sykes BD (1995) H-1, C-13 and N-15 random coil NMR chemical-shifts of the common amino-acids.1. Investigations of nearest-neighbor effects. *J Biomol NMR* 5(1):67–81
- Yang D, Kay LE (1999) Improved lineshape and sensitivity in the HNCO-family of triple resonance experiments. *J Biomol NMR* 14(3):273–276
- Yao J, Dyson HJ, Wright PE (1997) Chemical shift dispersion and secondary structure prediction in unfolded and partly folded proteins. *FEBS Lett* 419(2–3):285–289